Deformation correction for image-guided liver surgery: An intraoperative assessment of fidelity

Logan W. Clements, PhD,[a] **Jarrod A. Collins, BS,**[a] **Jared A. Weis, PhD,**[a] **Amber L. Simpson, PhD,**[b] **T. Peter Kingham, MD,**[b] **William R. Jarnagin, MD,**[b] *and* **Michael I. Miga, PhD,**[a] *Nashville, TN, and New York, NY*

Background. *Although systems of 3-dimensional image-guided surgery are a valuable adjunct across numerous procedures, differences in organ shape between that reflected in the preoperative image data and the intraoperative state can compromise the fidelity of such guidance based on the image. In this work, we assessed in real time a novel, 3-dimensional image-guided operation platform that incorporates soft tissue deformation.*

Methods. *A series of 125 alignment evaluations were performed across 20 patients. During the operation, the surgeon assessed the liver by swabbing an optically tracked stylus over the liver surface and viewing the image-guided operation display. Each patient had approximately 6 intraoperative comparative evaluations. For each assessment, 1 of only 2 types of alignments were considered: conventional rigid and novel deformable. The series of alignment types used was randomized and blinded to the surgeon. The surgeon provided a rating, R, from −3 to +3 for each display compared with the previous display, whereby a negative rating indicated degradation in fidelity and a positive rating an improvement.*

Results. *A statistical analysis of the series of rating data by the clinician indicated that the surgeons were able to perceive an improvement (defined as a $R > 1$) of the model-based registration over the rigid registration (P = .01) as well as a degradation (defined as $R < -1$) when the rigid registration was compared with the novel deformable guidance information (P = .03).*

Conclusion. *This study provides evidence of the benefit of deformation correction in providing an accurate location for the liver for use in image-guided surgery systems. (Surgery 2017;■:■-■.)*

From the Department of Biomedical Engineering,[a] *Vanderbilt University, Nashville, TN; and Department of Surgery,*[b] *Memorial Sloan-Kettering Cancer Center, New York, NY*

Hepatic tumors are localized routinely using preoperative diagnostic imaging (computed tomography or magnetic resonance imaging) combined with intraoperative ultrasonography, which surgeons fuse mentally during resection. High-resolution tomographic images acquired as standard of care for diagnosis and surgical planning complement the lesser resolution real-time capabilities of intraoperative ultrasongraphy. In patients treated with neoadjuvant chemotherapy, ultrasonography can fail to localize tumors due to differences in echogeneity in the presence of fatty liver disease[1] and can fail to detect differences in normal and ablated tissue.[2] Image-guided surgery attempts to address the limitations of both imaging modalities by providing real-time fusion and display of these data. Our group has performed fundamental research and development toward a Food & Drug Administration-approved, 3-dimensional (3-D) surgical navigation system to facilitate intraoperative guidance using fused preoperative tomographic and ultrasonnographic images.[3-5]

Guidance system overview. The goal of 3-D operative navigation systems is to facilitate the interactive use of preoperative tomographic imaging data during the operative procedure.

Supported by NIH grants R01-CA162477 and R01-NS049251.

Accepted for publication April 11, 2017.

Reprint requests: Logan W. Clements, PhD, Department of Biomedical Engineering, 5824 Stevenson Center, Nashville, TN 37232. E-mail: logan.clements@vanderbilt.edu.

0039-6060/$ - see front matter

http://dx.doi.org/10.1016/j.surg.2017.04.020

Fig 1. Screen captures of the software interfaces of the Scout Liver planning (top left) and Explorer Liver surgical navigation system (bottom left) are shown in addition to an image of the primary hardware associated with the Explorer Liver 3-D surgical navigation system (right panel).

To summarize, image-guided surgery (IGS) systems are comprised of 3 primary components: (i) preoperative image acquisition and processing, (ii) intraoperative instrument tracking, and (iii) alignment (ie, registration) and display of preoperative images in reference to the patient in real-time using the tracking technology. Only 2 Food & Drug Administration-approved, image-guided liver surgery systems exist: Fig 1 highlights the display and hardware components of the Explorer surgical navigation system (Analogic Corporation, Peabody, MA) for open hepatic operation described previously.[6-8] CAS-One (CAScination, Bern, Switzerland) is a similar system described by Peterhans et al.[9]

Image-guidance is the standard of care in neurosurgery,[10-12] but adoption in the liver has been hindered to due to the assumption that the liver is rigidly fixed.[13] More specifically, commercially available systems assume that the geometries of the preoperative anatomy represented in preoperative image volumes are preserved exactly within the intraoperative presentation counterpart, ie, no shape change. In the case of open hepatic surgery, this assumption is not valid due to the impact of the laparotomy incision, retraction, and mobilization of the organ prior to resection. The effect is that placing a tracked instrument on the physical tissue would result in the corresponding location within the image display being positioned incorrectly. For example, while an operative path designated in the guidance system may be clear with respect to moving past an important subsurface vessel, intraoperative deformation may compromise the fidelity of this guidance such that the path is not truly clear. A number of promising methods have been proposed to compensate for the impact of deformation on the fidelity of guidance information provided by 3-D IGS systems.[4,5,14] Although extensive work has been performed to evaluate the proposed models of deformation compensation, real time, intraoperative assessment of improvement with deformation compensation has yet to be evaluated by anyone in the field.

Contribution. In this work, we report on a novel, bystander study design tested >20 patient cases that to our knowledge has not been reported by other investigators. Specifically, we developed a real-time, deformation-corrected, image-guided system for liver operation modified to allow for multiple display evaluations during an operation. The study

Table I. Summary of the demographic, pathologic, and intraoperative information for the patients enrolled in this IRB-approved clinical study performed at Memorial Sloan-Kettering Cancer Center

Patient	*Sex*	*Age*	*Weight (kg)*	*Height (cm)*	*Pathology*	*Procedure*
1	M	53	130.8	184	Gallbladder, cancer	Wedge biopsy
2	M	55	144.7	194	Metastatic cancer, colorectal	Right lobectomy
3	F	55	59	156	Metastatic cancer, fallopian	Segmentectomy, 6
4	M	39	73	167	Metastatic cancer, colorectal	Right lobectomy
5	F	54	59.4	166	Biliary, peripheral cholangiocarcinoma	Left trisegmentectomy
6	F	77	74.4	148	Metastatic cancer, colorectal	Left lateral segmentectomy
7	F	69	53.7	155	Gallbladder, cholelithiasis	Liver biopsy, wedge
8	M	49	78.6	171	Metastatic cancer, colorectal	Segmentectomy, 8
9	M	69	94	183	Biliary, peripheral cholangiocarcinoma	Bile duct resection
10	M	56	71.1	182	Metastatic cancer, colorectal	Segmentectomy, 5
11	F	79	58.5	150	Biliary, cholangitis	Right trisegmentectomy
12	F	51	49	157.5	Metastatic cancer, colorectal	Segmentectomy, 3
13	F	79	43.5	154	Metastatic cancer, colorectal	Segmentectomy, 4a/8
14	F	74	85.3	155	Metastatic cancer, Colorectal	Right posterior sectorectomy
15	F	52	80.7	163	Metastatic cancer, colorectal	Hepatic artery infusion pump Placement
16	M	54	127.5	181	Metastatic cancer, colorectal	Segmentectomy 4b
17	M	56	87.1	184	Metastatic cancer, colorectal	Caudate lobectomy
18	F	54	55.5	160	Metastatic cancer, colorectal	Wedge resection segments 3, 4a, 6, 8, 5 (x2)
19	F	69	76.7	145	Intrahepatic cholangiocarcinoma	Right hepatic trisectionectomy
20	F	66	73.3	152	Metastatic cancer, colorectal	Segmentectomy, 5 and 6

The study population included 20 patients operated on by 2 surgeons for which a total of 125 evaluations of navigation accuracy were performed.
IRB, Institutional review board.

entailed the evaluation of 2 display types: a display using a conventional rigid alignment, and a second using our deformation corrected alignment. During the operation, a minimum of 6, sequential, comparative evaluations with the display types being selected in a randomized blinded manner were performed. Using standard techniques of intraoperative interrogation (swabbing of the organ and observing the corresponding guidance display), the surgeon rated the fidelity of each display in reference to the previous display. For the purposes of this work, fidelity of the display refers to the extent to which the guidance information displayed by the 3-D IGS system corresponds with the known location of the tracked instrumentation on the organ during the procedure. A rating range was used, such that the extent of improvement or degradation could be recorded, as well as detecting no change. The ratings were then correlated with order of display evaluations, and a quantitative evaluation of the fidelity of improvement was determined.

METHODS

For this study, a series of evaluations of the guidance systems were performed for 20 patients undergoing open liver resection at Memorial Sloan Kettering Cancer Center (MSKCC). The patients provided written consent to be included in the study that was approved by the MSKCC Institutional Review Board. A summary of the demographic information for the patients enrolled in the study is shown in Table I, and 2 practicing hepatobiliary surgeons participated (W.R.J., $N = 13$ and T.P.K., $N = 7$).

Overall, the study involved 3 primary steps: (i) preoperative image acquisition and processing, (ii) intraoperative registration and evaluation, and (iii) then a postoperative statistical analysis. The intraoperative registration evaluation involved the blinded display, randomized-to-surgeon of 2 alignment types for computing the requisite mapping between the intraoperative presentation of the patient anatomy and the preoperative image data. The order of registrations displayed was blinded to the clinician and system operator of the surgical navigation system. We should note that comparative evaluations where the display type transitioned from rigid-to-deformable or deformable-to-rigid were sampled a similar number of times and more extensively than instances when a display would remain the same. It should

be noted, however, that in the randomization process, we ensured that the display was held constant at least once and often more than once for each patient evaluation. The rationale for this approach is that many evaluations while the patient is under anesthesia can problematic, and as a result, these constraints to the selection process of random display were appropriate. Nevertheless, display distributions were determined by the Vanderbilt team (L.W.C., J.A.C., J.A.W., and M.I.M.) in randomized fashion and distribution strategy, while the order of evaluation was kept blinded strictly to the test site, MSKCC.

Preoperative image processing. Standard contrast-enhanced CT images were acquired for all patients prior to the operative procedure. In order for the tomographic images to be utilized within the 3-D image guidance system, a preoperative processing and planning step was required. The series of contrast-enhanced tomographic images were imported into the Scout Liver (Analogic Corporation) software package, and 3-D anatomic models of the liver, tumor(s), and vascular structures were generated via a series of semiautomated algorithms. A summary of the methods used in the preoperative planning software and an evaluation of the impact of the planning software has been published previously.[15,16]

Intraoperative guidance and data collection. After the preoperative image processing of the image data had been performed, the Scout Liver software was used to export the tomographic images and 3-D models for us in a modified surgical guidance system (Explorer Liver, Analogic Corporation). As mentioned previously, the display of tracked instrumentation on the preoperative tomograms and anatomic models required a mathematic mapping or registration between the intraoperative presentation of the patient (ie, "patient space") and the presentation of the patient anatomy in the preoperative tomograms (ie, "image space"). For the purposes of this evaluation, 2 different registration methods were used: a conventional rigid registration and our novel deformable registration. It should be noted that the modified Explorer Liver guidance system was not used for guidance during the performance of the surgical procedures and was used only for the purposes of registration evaluation.

Summary of registration methods. The conventional registration method used in commercial 3-D surgical navigation systems (eg, StealthStation, Medtronic PLC, Dublin, Ireland) for aligning the intraoperative presentation and the preoperative image space assumes that the patient anatomy is rigid. These rigid registration techniques allow for extremely rapid computation of the mathematic transformation that links the intraoperative patient space to the preoperative image space. For IGS application to the liver, alignment routines use the preoperative 3-D surface of the liver generated from the preoperative planning software and the counterpart surface acquired in the operating room by the clinician with an optically tracked probe. Briefly, the location of the probe is recorded continuously as the surgeon swabs the organ surface, and a representative sampling of the visible surface is constructed. The details of the registration method used in the Explorer Liver system have been described in the work of Clements et al.[17]

As opposed to rigid registration system, the second registration type used in this study was a deformable registration method and involved the use of a mathematically adjustable, anterior liver support surface that can capture dynamically the manipulation of the organ performed after laparotomy. The controlling parameters are determined via an optimization routine described and validated in previous work.[14]

Intraoperative performance and evaluation of registration. After the laparotomy and mobilization, the liver was prepared such that movement was limited via placement of surgical sponges. At this point, conventionally, the surgeon then uses the optically tracked probe to swab across the exposed surface of the liver to facilitate rigid registration. As reported,[17] rigid registration for liver IGS is a process whereby the falciform ligament, round ligament, and inferior ridges are localized on both a segmented virtual organ from CT images and within the operating room on the physical patient using a tracked stylus. After the surface data are collected by the surgeon, registration is performed by aligning surfaces. The fidelity of this guidance can be reviewed to ensure that additional data collection is not needed. The review process of the fidelity of the guidance generally involves the placing of the tracked probe at various locations on the organ surface that can be identified reliably in the preoperative image data and then observing the guidance system display output.

Once the initial rigid registration has been calculated and accepted by the surgeon, computation of the deformable registration is then performed. The calculation of the deformable registration requires approximately 2 minutes to complete. After completion of the calculation, the Explorer Liver system selected a display to evaluate

based on a randomized order generated by the Vanderbilt team and as part of the blinded evaluation process that took place at MSKCC.

With each display provided sequentially to the MSKCC evaluating surgeon, a conventional assessment of fidelity was conducted, ie, while swabbing the open liver surface, the alignment was evaluated for correspondence on the display of known structures. Each display was evaluated for approximately 30 seconds with the first 10 seconds being recorded for purposes of data analysis. After completion, the surgeon was asked to provide a rating, *R*, on a +3 to −3 scale whether the display being evaluated was better or worse regarding accuracy using a known spot on the liver. The rating compared the new and previous image, where 0, +1, +2, +3 represented ratings of no improvement, small, moderate, and highly improved, respectively. The negative ratings were similar but reflect worsening. The comparison and rating process proceeded until at least six comparative evaluations had been performed. Additional ratings were performed by the surgeon as time permitted.

Postoperative evaluation. The postoperative evaluation of the collected clinical data first required the extraction of the order of registration evaluations, the series of ratings of guidance quality, and the recorded location of the tracked probe during the registration evaluation. The guidance quality rating data was separated into 3 groups based on the order of registration methods used: (i) comparing the deformable registration to the previous rigid registration, (ii) comparing the rigid registration to the previous deformable registration, and (iii) the scenario where there was no change in the registration displayed (ie, a deformable followed by a deformable registration). Once the ratings had been separated into the 3 categories, a series of continuous statistics was computed (ie, mean, standard deviation, and median) and a series of statistical tests were performed.

The data recorded from the tracked probe for each registration evaluation also was used to compute metrics of distance for providing a quantitative approximation of the accuracy of the surgical navigation. In this work, the average Euclidean distance between the location of the tracked probe and the 3-D organ surface based on the registration method used in the evaluation was utilized. After the individual Euclidean distances were computed for each individual display evaluation, the difference in the Euclidean distance between subsequent displays was computed. More specifically, the Euclidean distance computed for a current registration evaluation was subtracted from the Euclidean distance computed for the previous registration evaluation. The correlation of the metric changes in distance in reference to ratings then were analyzed. As an example, in a scenario where the surgeon evaluated a display where the registration was of the rigid type, and then a subsequent display used the deformable type, one would expect an improvement in the rating of fidelity and for the difference in the Euclidean, distance to be positive, because the distance between probe and image-derived organ surface would be greater in the rigid type evaluation than in the deformable context. One can see this in Fig 2 by observing d_1 and d_2 in Acquisition 1 and Acquisition 2, respectively, where clearly $d_1 > d_2$, which would result in a positive difference in the Euclidean distance as $d_1–d_2 > 0$. The difference itself is reported in the second row, third column of embedded legend table.

Once all of the difference values in the Euclidean closest point distance were computed, these distance measurements were used for statistical comparison. Similar to the ratings, the distance measurements were collected into the same groupings: (i) comparison of deformable registration to the previous rigid registration, (ii) comparison of the rigid to the previous deformable registration, and (ii) no change in registration display. It should be noted that there are fewer measurements of distance difference than total measurements of registration rating because the location of the probe was not recorded during the initial evaluation of the rigid registration during which time the deformable registration was computed. Furthermore, there were 3 additional 10 second evaluation periods where nonevaluable data of the tracked probe were recorded due to problems of the online of sight with the optical tracking system.

Summary of statistical methods. To measure the ability of the surgeon to detect improvement or degradation, the Wilcoxon signed-rank test was used to evaluate each of the data series of guidance rating by the surgeon across the three display scenarios. For these tests, we defined a perceived clinically important improvement in guidance accuracy as a rating greater than +1. Similarly, a clinically important degradation in guidance accuracy was a rating less than −1. Therefore, any rating that is between −1 and +1, inclusive, corresponded to no perceived, clinically important change in accuracy of guidance.

Additionally, the Wilcoxon rank-sum test was used to perform direct statistical comparisons between each of the 3 series of ranking data for the 3 different scenarios of registration display. as well as for comparisons between the probe-to-surface data

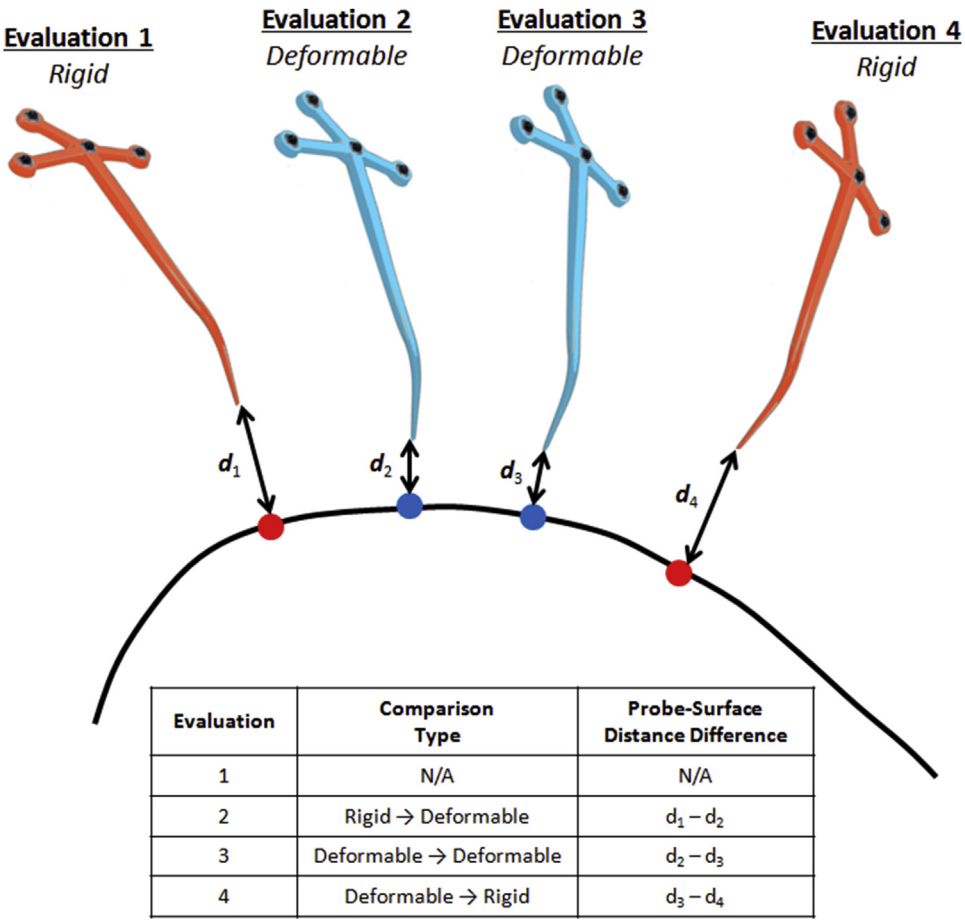

Evaluation	Comparison Type	Probe-Surface Distance Difference
1	N/A	N/A
2	Rigid → Deformable	$d_1 - d_2$
3	Deformable → Deformable	$d_2 - d_3$
4	Deformable → Rigid	$d_3 - d_4$

Fig 2. Visualization of the calculation metric of the closest point distance used to quantify the difference in guidance information provided by the 2 registration methods as well as to analyze the consistency of the clinician rating data. A series of 4 registration evaluations are visualized, where the 2 evaluations of the rigid registrations are shown as the *orange* tracked probes and the 2 deformable registrations are shown with the *blue* tracked probes. Each of the distances (*d*) indicates the Euclidean distance between the tip of the tracked probe and the corresponding closest point on the liver surface (*curved black line*). For each of the evaluations, the closest point on the liver surface is represented as a *sphere* where the organ *sphere* corresponds with the rigid registration evaluation and the *blue spheres* correspond with the deformable registration evaluations.

of distance difference grouped together via 2 different methods. Specifically, statistical comparisons were performed where the probe-to-surface distance difference measurements were compiled based on the order of registration evaluation according to the order of the blinded display and then subsequently according to the levels of detected clinically important improvement in guidance accuracy (ie, $R > 1$), a perceived clinically important degradation in accuracy (ie, $R < -1$), and no perceived clinically important change (ie, $|R| \leq 1$).

RESULTS

Visualizations of the surface alignments computed within the 2 registration methods for a series of patients is shown in Fig 3. On the left (Fig 3, *A* to *C*), the color map shows a distribution of Euclidean distances using the rigid-type registration (ie, red indicates the image-derived model surface is approximately 15 mm above the registered data, and blue would 15 mm positioned below the data). On the right (Fig 3, *D* to *F*), the color map shows the corresponding respective equivalent metric but after the deformable-type registration. Although Fig 3 provides some quantitative demonstration of improved alignment, Fig 4 presents a more practical visualization with the guidance system in use. The visualizations highlight panels showing a crosshair overlay in the tomographic guidance display as well as a 3-D rendering of the location of the tracked probe used for data collection and registration

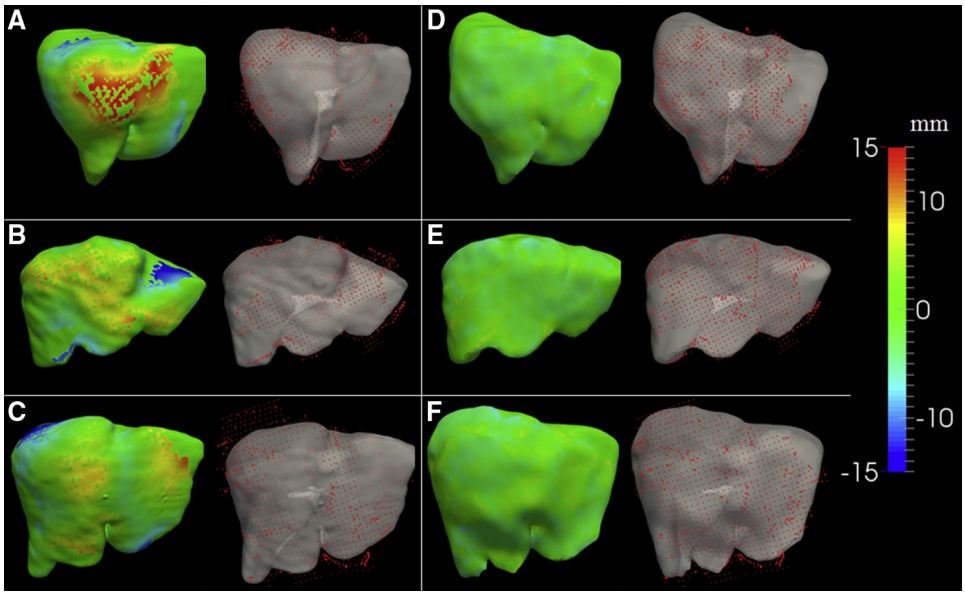

Fig 3. Visualization of the registration results provided by the 2 registration methods evaluated for 3 patients in the study. *A* to *C* show a series of visualizations of the registration alignments for the rigid registration, while the *D* to *F* provide visualizations of the deformable registration. The color-mapped, 3-D organ surface on the left side of each panel represents the signed closest-point distance between the intraoperatively acquired data of the liver surface (*red points*), and the 3-D model of the organ derived from the preoperative tomograms (*grey surface*).

evaluation. It should be noted that the probe in all cases was placed on the physical surface of the organ. As shown, there is a noticeable improvement in the guidance information displayed for the deformable registration compared with the rigid registration. The conventional displays show the location deep within the tissue for one patient (Fig 4, *A* left column), and floating above the liver in the second patient (Fig 4, *B*, left column). The corrected display shows the crosshairs on the organ surface for each (Fig 4, *A* and *B*, right column), which is the true physical state intraoperatively.

A series of histograms of the registration rating data acquired in this study is shown in Fig 5. A total of 125 registration evaluations were performed throughout the entire 20 patient cohort. The histograms are separated based on the type of registration comparison performed: (i) comparative registration evaluations of deformable registration to previous rigid registration (Fig 5, *A*) (ii) comparative registration evaluations of rigid registration to previous deformable registration (Fig 5, *B*), and (iii) no change in registration display (Fig 5, *C*). The patterns exhibited by the 3 histograms indicate that the surgeons tended to: (1) rate an improvement in guidance information (ie, positive rating value) when evaluating the deformable-type registration when the previous was rigid-type, (2) rate a degradation (ie, negative rating value) when evaluating the rigid-type registration when the previous registration system was the deformable-type, and (3) rated no change (ie, value of zero) when comparing types of the same registration.

In addition to the histogram visualizations, a statistical summary is shown in Table II and highlights the clinician rating data, the corresponding Wilcoxon signed-rank tests associated with the ranking data, and the mean differences in probe-surface distances for each comparison type. As expected from the histogram visualizations, the comparisons associated with evaluating the deformable-type registration when the previous registration system was rigid-type resulted in a mean rating of +1.5, an improvement in fidelity, and the comparisons associated with evaluating the rigid-type registration when the previous was deformable-type resulted in a mean rating of −1.4, a degradation in fidelity. The statistical significance of the improvement comparison was provided via a right-sided Wilcoxon signed-rank test which established if the median of the ranking data was greater than +1. With the *P* value of .01, the null hypothesis is rejected, and the median value of the rating series collected with this comparison was greater than +1 with statistical significance.

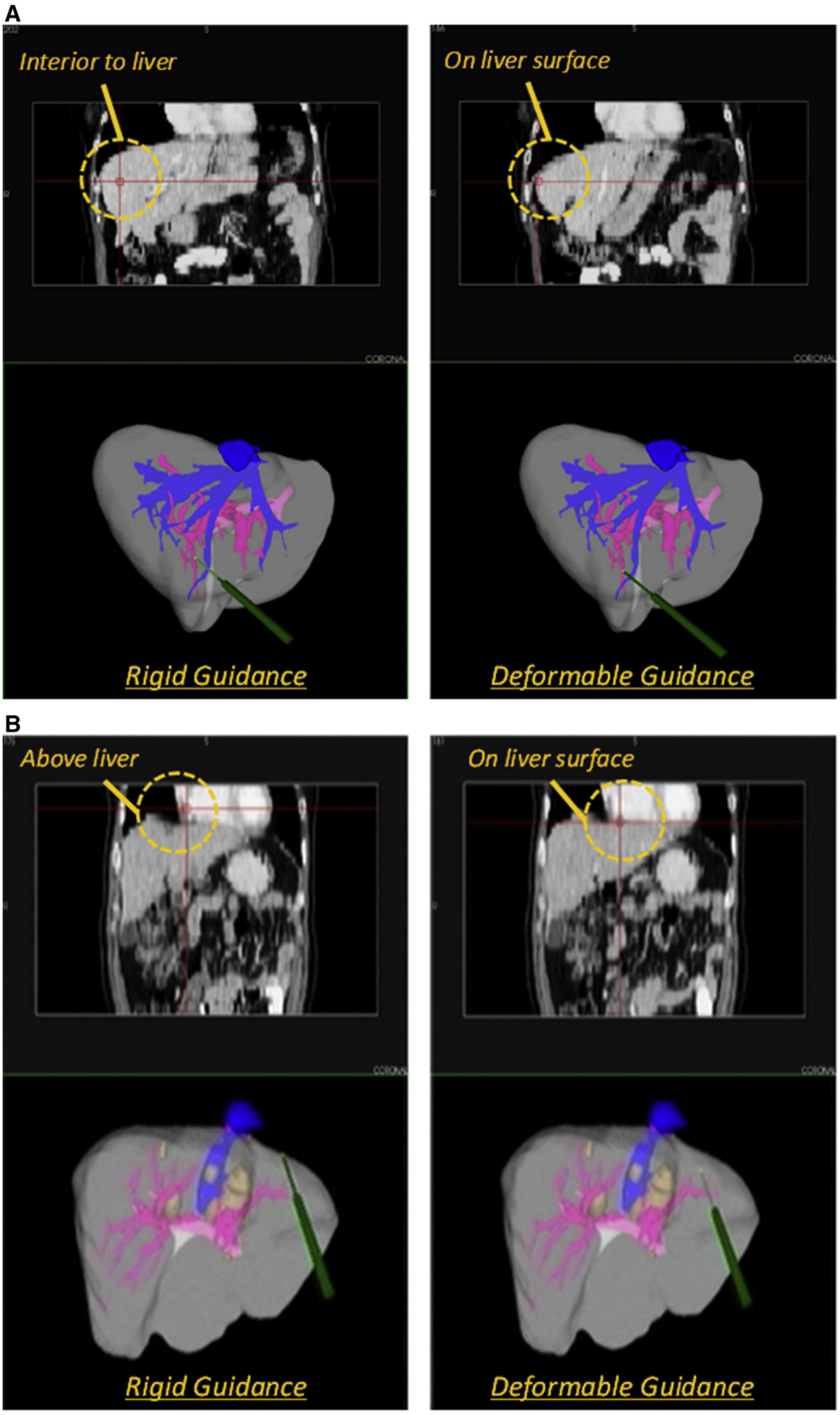

Fig 4. Sample visualizations of the guidance information provided by the 2 registration methods taken from 2 of the panels of the display configuration used in the modified Explorer Liver surgical navigation system for (*A*) Patient 11 and (*B*) Patient 17. Note, the display includes the tomographic display of the coronal plane as well as the 3-D render window that includes the 3-D anatomic models; the stylus is on the physical organ surface when display data were collected. The left column is based on rigid guidance, and right column is deformation corrected. *Orange* call-outs are provided.

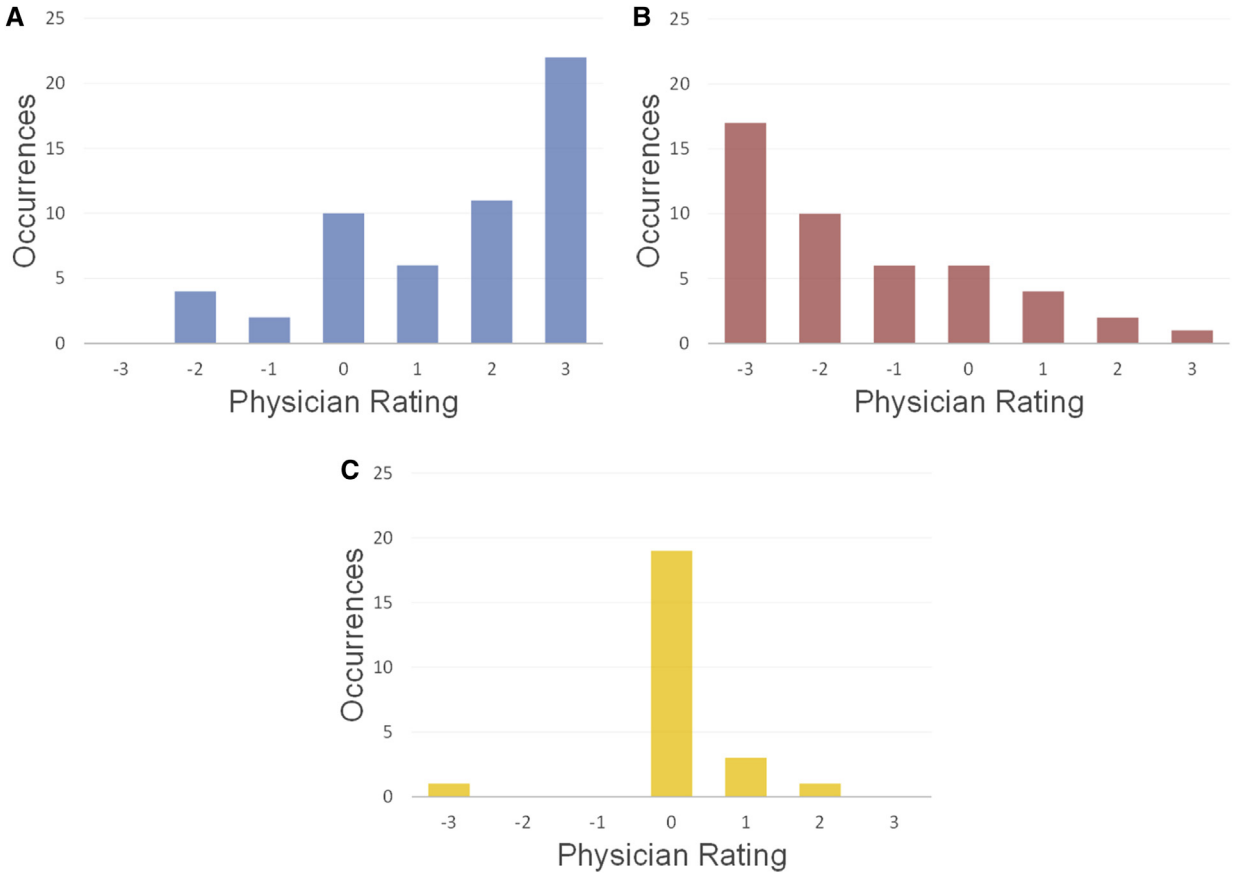

Fig 5. Histogram visualization of the data obtained by surgeon ranking performed across the 125 registration evaluations for the full patient population. The histograms have been separated based on the 3 different categories of comparison: (*A*) comparing the deformable registration to the previous rigid registration, (*B*) comparing the rigid registration to the previous deformable registration, and (*C*) the scenario where there was no change in the registration displayed.

Table II. A statistical summary of the rating values (*R*) of the registration evaluation compiled across the entire patient population and mean differences in probe-surface distance

Comparison	*Sample size* (N)	*Rating value (R) (mean ± SD [median])*	*Wilcoxon signed-rank test*	*Sample size* (N)	*Mean probe-surface distance difference (mean ± SD [median] mm)*
Rigid → Deformable	55	1.53 ± 1.60 [2.0]	H_1: $R > 1$; $P = .01$	44	3.04 ± 4.15 [1.57]
Deformable → Rigid	46	−1.43 ± 1.67 [–2.0]	H_1: $R < -1$; $P = .03$	45	−3.72 ± 4.26 [–2.29]
Same method	24	0.08 ± 0.83 [0.0]	H_1: $R \neq 0$; $P = .56$	12	−0.72 ± 2.94 [0.01]

The physician evaluations are grouped into 3 categories of comparison: (i) comparing the deformable registration to the previous rigid registration, (ii) comparing the rigid registration to the previous deformable registration, and (iii) the scenario where there was no change in the registration displayed. Wilcoxon signed-rank tests were used to evaluate the ability of the clinicians to perceive clinically important improvements ($R > 1$) when the deformable registration was compared with the previous rigid registration, the ability of the clinicians to perceived clinically important degradation ($R < -1$) when the rigid registration was compared with the previous deformable registration, and the consistency in perception of the clinician in the cases where the same registration methods were compared and no clinically important change ($|R| \leq 1$) in guidance accuracy should occur. Additionally, not reported in the table, the Wilcoxon rank-sum test was used to compare each of the 3 groups of data of distance difference with each other and resulted in differences for all comparisons ($P < .05$).

Similarly, a left-sided Wilcoxon signed-rank test was used to establish the existence of a degradation (ie, rating value less than −1). The resulting P value of .03 indicates that the null hypothesis was rejected, and the median value of the rating series collected with this comparison was less than −1 with statistical significance. Finally, a 2-sided Wilcoxon signed-rank test was used to test whether or not the median value of the ratings collected when comparing a sequence of same-type registration displays varied significantly from zero. As indicated, the P value of .56 indicates that the null hypothesis was accepted, and the median rating value of the comparisons of the same registration was no different than zero.

With respect to the last column of Table II, the mean difference in the Euclidean distances in the scenario of evaluating the deformable registration when the previous was rigid-type was found to be 3.0 mm. This states that the average distance between the probe and surface decreased by approximately 3.0 mm when transitioning from a display using rigid registration to one using the deformable method. Similarly, the mean difference in the Euclidean distances in evaluating the rigid registration when the previous was deformable-type resulted in Euclidean distance difference of −3.7 mm, thus reflecting an increase in the distance between the probe and surface when transitioning from a display using deformable registration to one using the rigid method. Finally, the mean difference in the Euclidean distances when the same registration methods were compared with the sequence was found to be −0.7 mm, which reflects the consistency of the distance between the probe and 3-D organ surface as displayed within the guidance system with same-type registrations.

To add some further analysis of Table II data, we parsed the data further to specifically meet the significance tests for ratings of improvement, degradation, and no change, ie, $R>1$ (N = 28), $R< -1$ (N = 32), and $|R|\leq 1$ (N = 41), respectively. When parsing the data in this manner, the mean difference in the Euclidean distances became 4.1 mm for $R > 1$ rather than raw analysis value of 3.0 mm. In other words, the distance between the probe and surface during the evaluation was approximately 4 mm closer to the organ surface on average when the clinician perceived a clinically important improvement in guidance. Similarly, when a clinically important degradation in guidance was perceived, ie, $R < -1$, the mean difference in the Euclidean distances was −4.6 mm versus −3.7 mm in the raw analysis. Finally, in the situation where no change in guidance information was perceived, ie, $|R| \leq 1$, the mean difference in the Euclidean distances was −0.3 mm vs −0.7 mm.

DISCUSSION

The results of this study indicate that the participating surgeons quantitatively reported a statistically significant and clinically important improved fidelity in the guidance display utilizing our novel deformable registration approach over the conventional rigid approach. When display types were held constant, surgeons also quantitatively reported no change in the fidelity of guidance. In addition, the assessment of fidelity was also consistent with the increase or decrease in quantitative physical measurements associated with Euclidean distances made but the probe positioning during the registration evaluation (summarized in last column of Table II). Equally encouraging is the lack of change of the metrics of Euclidean distance when the displays did not change.

Although the data of Euclidean distance computed from the tracked recordings of the probe during the registration evaluations provided quantitative comparison, the extent of that validation is limited to surface distances and does not reflect an absolute calculation of guidance error. More specifically, it is only possible to know how close the probe is displayed to the organ surface within the context of the guidance system, but not possible to know the true distance between the point at which the probe is held on the surface within the operating room environment and the "true" corresponding point within the image data. It also then follows that the work does not report any information regarding error of subsurface localization of surgical targets.

Although intraoperative validation of subsurface target error was outside the scope of this work, several other studies have been performed retrospectively using both phantom and clinical data to determine subsurface target errors associated with the deformable registration method used in this study. The work of Rucker et al, which was the first published description of the deformable registration method, involved the performance of several validation experiments using an anthropomorphic phantom to evaluate errors with respect to sub-surface targets.[14] The presented method decreased the volumetric error from an average root mean square error of 9.5 mm after standard rigid registration to 3.3 mm after deformable registration. Further validation efforts also were performed using tracked ultrasonographic data recorded during open hepatic operations.[18]

In this work, the framework of the deformable registration was used in a 6 patient study that used data from the anterior surface and the registration technique to predict the location of subsurface vascular targets. Using tracked ultrasonnographic imaging, these targets could then be compared with their preoperative imaged counterpart with and without correction. The findings demonstrated a decrease in the subsurface target feature error from 5.6 ± 2.2 mm to 2.7 ± 0.7 mm after correction, an approximate 52% correction.

Nevertheless, this work represents the first report of a randomized, blinded, intraoperative study of the assessment of the guidance fidelity by several surgeons. Based on this work, we would suggest consideration of a paradigm shift in the field of soft-tissue image guidance. The data is supportive that deformation correction is a detectable phenomenon within IGS systems. These results imply that the proposed deformable registration technique holds substantial promise in improving the guidance information provided to clinicians during open hepatic procedures in what may be a cost-effective manner.

This work was supported under the NIH grants R01-CA162477 and R01-NS049251. The authors would like to thank Dr Hakmook Kang of the Vanderbilt University Department of Biostatistics for consultation on the statistical analysis performed in this work. Many of the rendered surfaces shown in this work were generated using the Visualization Toolkit (Kitware Inc., Clifton Park, NY; https://www.vtk.org) and the ParaView software package (Kitware Inc., Clifton Park, NY; https://www.paraview.org) was used for screen shot captures used in a number of the figures. Additionally, the statistical tests were run via MATLAB (The MathWorks Inc., Natick, MA; https://www.mathworks.com/).

REFERENCES

1. van Vledder MG, Torbenson MS, Pawlik TM, Boctor EM, Hamper UM, Olino K, et al. The effect of steatosis on echogenicity of colorectal liver metastases on intraoperative ultrasonography. Arch Surg 2010;145:661-7.
2. Bilchick AJ, Krasny RM, Allegra D. Radiofrequency ablation for liver tumors. In: Jarnagin WR, editor. Blumgart's Surg Liver, Biliary Tract, Pancreas, 5th ed. Philadelphia, PA: Elsevier; 2012.
3. Cash DM, Miga MI, Glasgow SC, Dawant BM, Clements LW, Cao Z, et al. Concepts and preliminary data toward the realization of image-guided liver surgery. J Gastrointest Surg 2007;11:844-59.
4. Cash DM, Miga MI, Sinha TK, Galloway RL, Chapman WC. Compensating for intraoperative soft-tissue deformations using incomplete surface data and finite elements. IEEE Trans Med Imaging 2005;24:1479-91.
5. Miga MI, Cash DM, Cao Z, Galloway JR, Dawant BM, Chapman WC. Intraoperative registration of the liver for image-guided surgery using laser range scanning and deformable models. Medical imaging 2003: visualization, image-guided procedures, and display. San Diego, CA: Proc SPIE; 2003:350-9.
6. Kingham TP, Scherer MA, Neese BW, Clements LW, Stefansic JD, Jarnagin WR. Image-guided liver surgery: intraoperative projection of computed tomography images utilizing tracked ultrasound. HPB (Oxford) 2012;14:594-603.
7. Kingham TP, Jayaraman S, Clements LW, Scherer MA, Stefansic JD, Jarnagin WR. Evolution of image-guided liver surgery: transition from open to laparoscopic procedures. J Gastrointest Surg 2013;17:1274-82.
8. Simpson AL, Kingham TP. Current evidence in image-guided liver surgery. J Gastrointest Surg 2016;20:1265-9.
9. Peterhans M, vom Berg A, Dagon B, Inderbitzin D, Baur C, Candinas D, et al. A navigation system for open liver surgery: design, workflow and first clinical applications. Int J Med Robot 2011;7:7-16.
10. Kondziolka D, Lunsford LD. Intraoperative navigation during resection of brain metastases. Neurosurg Clin N Am 1996;7:267-77.
11. Korinth MC, Delonge C, Hütter BO, Gilsbach JM. Prognostic factors for patients with microsurgically resected brain metastases. Oncol Res Treatment 2002;25:420-5.
12. Paleologos TS, Wadley JP, Kitchen ND, Thomas DG. Clinical utility and cost-effectiveness of interactive image-guided craniotomy: clinical comparison between conventional and image-guided meningioma surgery. Neurosurgery 2000;47:40-7; discussion 7-8.
13. Clements LW, Dumpuri P, Chapman WC, Dawant BM, Galloway RL, Miga MI. Organ surface deformation measurement and analysis in open hepatic surgery: method and preliminary results from 12 clinical cases. IEEE Trans Biomed Eng 2011;58.
14. Rucker D, Wu Y, Clements L, Ondrake J, Pheiffer T, Simpson A, et al. A mechanics-based nonrigid registration method for liver surgery using sparse intraoperative data. IEEE Trans Med Imaging 2014;33:147-58.
15. Li S, Waite JM, Lennon BT, Stefansic JD, Li R, Dawant BM. Development of preoperative liver and vascular system segmentation and modeling tool for image-guided surgery and surgical planning. Medical imaging 2008: visualization, image-guided procedures, and modeling. San Diego, CA: Proc. SPIE; 2008. 9180C-C-8.
16. DuBray BJ Jr, Levy RV, Balachandran P, Conzen KD, Upadhya GA, Anderson CD, et al. Novel three-dimensional imaging technique improves the accuracy of hepatic volumetric assessment. HPB (Oxford) 2011;13:670-4.
17. Clements LW, Chapman WC, Dawant BM, Galloway RL Jr, Miga MI. Robust surface registration using salient anatomical features for image-guided liver surgery: algorithm and validation. Med Phys 2008;35:2528-40.
18. Clements LW, Collins JA, Weis JA, Simpson AL, Adams LB, Jarnagin WR, et al. Evaluation of model-based deformation correction in image-guided liver surgery via tracked intraoperative ultrasound. J Med Imaging (Bellingham) 2016;3:015003.